EJECTOR SUBASSEMBLY FOR DUAL WALL AIR DRILLING

TEMPRESS® TECHNOLOGIES, INC.

Jack Kollé
Principal
Dynamic Fluid Systems Development

P.O. Box 80384
637 South Lucile St.
Seattle, WA 98108-0384
1.800.426.2600
TEL 206.762.1410
FAX 206.762.1859

INTRODUCTION

The dry drilling system developed for the Yucca Mountain Site Characterization Project incorporates a surface vacuum system to prevent drilling air and cuttings from contaminating the borehole wall during coring operations (Long et al., 1992). As the drilling depth increases, however there is a potential for borehole contamination because of the limited volume of air which can be removed by the vacuum system. A feasibility analysis (Kolle, 1993) has shown that an ejector subassembly mounted in the drill string above the core barrel could significantly enhance the depth capacity of the dry drilling system. The ejector subassembly would use a portion of the air supplied to the core bit to maintain a vacuum on the hole bottom. The results of a design study including performance testing of laboratory scale ejector simulator are presented here.

EJECTOR PERFORMANCE OBJECTIVES

Site characterization plans at the Yucca Mountain Project site call for drilling to a depth of 2500 ft (762 m) and anticipate drilling into wet and/or saturated formations. During coring all of the air and cuttings must flow in the annulus between the core rod and dual wall drill string as shown in Figure 1. At sufficient depth, a pressure differential will be established between the annulus and the hole bottom which could cause borehole contamination. During coring operations, 700 scfm of air at a pressure of 100 to 150 psi is delivered to the coring bit for cooling and cuttings removal. This air flows upwards in the annulus between the core rod and dual-wall drillstring. The vacuum system provides a differential pressure drop of 6.9 psid. The relationship between flow rate and pressure in the annulus can be found in Lyons (1984). Figure 2 shows the pressure in the annulus as a function of the annulus length at the maximum dry drilling system coring rate of 25 ft/hr. The static borehole pressure at the Yucca Mountain site (elevation = 6000 ft) is also shown as a function of borehole depth. Under these operating conditions the annulus pressure will exceed the static borehole pressure when the hole is deeper than 2000 ft. At this point, the annulus will no longer accept all of the 700 scfm delivered through the core bit and some of the air will blow by the reaming bit to contaminate the borehole .

Figure 3 shows the concept of an ejector subassembly mounted on the core rod just above the core barrel. During coring operations, part of the coring air is diverted through primary jets on the ejector and used to provide a pressure boost at the bottom of the dual wall drill string. The effect of a 20% pressure boost on the uncontaminated depth capacity of the dry drilling system is illustrated in Figure 2. Without the pressure boost, borehole contamination will occur at depths below 2000 ft. A 20% pressure boost would increase the depth capacity to 3300 ft. This level of pressure boost would also provide a much greater margin of safety at depths below 2000 ft and would compensate for leaks in the surface vacuum system or for surges in drilling rate which can cause pressures in the annulus between the core rod and dual wall to increase.

The ejector would use a portion of the coring air to provide the desired pressure boost. The dry drilling system is now designed to provide air lift velocities of around 6000 ft/min in the annulus between the dual wall and the core rod. If half of the coring air is used to drive the ejector, the standard air velocity is reduced to 3000 ft/min in the annulus beneath the subassembly. This air velocity is the minimum considered sufficient to lift rock cuttings (Angel, 1958). The performance objective for the ejector subassembly is thus to provide a pressure boost of 20% using less than half of the coring air.

SEGMENTED ANNULAR EJECTOR

A design for an ejector subassembly consisting of a number of two-dimensional ejector segments separated by stabilizer fins is shown in Figure 4. In this design, the dual wall inner diameter acts as one of the walls of the ejector mixing duct. This approach eliminates the need for seals between the ejector subassembly and the dual wall tube. While this design is well suited for downhole use, the annular ejector geometry introduces complexities in the flow which are difficult to model analytically.

EJECTOR SIZING

An ejector uses a primary jet at relatively high pressure to entrain a secondary flow and provide a pressure boost. A schematic of a constant area supersonic ejector is shown in Figure 5. Ejector performance is determined by the ratio of secondary to the primary air mass flow (mass flow ratio) and the ratio of dynamic pressure at the mixing duct exit to the secondary air pressure at the inlet (pressure ratio).

The performance of an ejector with fixed geometry is constrained to lie on the three dimensional surface depicted in Figure 6. We want to operate in the supersonic regime (SR) where the mass flow ratio is independent of pressure ratio. If the pressure ratio becomes too great, there is a steep drop in mass flow ratio in the mixed regime (MR). Ejector performance is optimized by constraining the design and operating parameters to be on the breakoff curve, *ab*. For optimum ejector designs which lie along this curve there is an inverse tradeoff between the mass flow ratio and the pressure ratio.

Ejector optimization was performed by iterating operating parameters using the CAEOPT3 (Constant Area Ejector Optimization) code developed by Dutton and his coworkers at the University of Illinois, Champaign-Urbana (Dutton and Carrol, 1986). This model uses a control volume approach to solve the equations of mass and momentum balance for isentropic gas flow. Duct friction and mixing losses are accounted for by an empirical pressure recovery coefficient for the ejector. Ejector performance predictions using this model have been verified by comparison with extensive experimental investigations. The performance model includes an empirical estimate of pressure recovery in the subsonic diffuser section based on an extensive compilation of diffuser performance data provided by Runstadler et al. (1975).

We assume a primary jet pressure of 120 to 150 psi, which is compatible with the existing coring air pressure. The secondary stagnation pressure at the hole bottom is assumed to be 12 psi. These values were used to size an ejector for operation at a mass flow ratio of 1 which corresponds to using half of the coring air to drive the primary. The design analysis showed that an optimal ejector could provide a 50% boost in system pressure if the air flow is evenly partitioned between the coring bit and the ejector subassembly.

The air compressors on the dry drilling system supply up to 900 cfm of air at the local surface atmospheric pressure of around 12 psia. This corresponds to approximately 700 scfm air. If half of the flow is diverted to the ejector primary flows of 350 scfm must entrain an equal secondary flow to prevent cuttings from escaping from around the reaming bit.

SIMULATOR DESIGN

In the design study described here a laboratory simulator consisting of one segment of a segmented annular ejector was fabricated and used to evaluate performance under conditions expected during coring operations. An instrumented compressed air flow system was developed to allow measurements of all of the critical parameters which describe ejector performance.

A schematic of the simulator and instrumentation is shown in Figure 7. Compressed air at a regulated pressure of up to 200 psia was supplied to the primary nozzle from a tank sized to provide 20 seconds of air at a flow rate of 60 scfm without a significant change in air supply pressure. A pressure transducer monitors the primary supply pressure. The primary air flow rate is calculated from the pressure and the size of the primary nozzle throat using the isentropic flow equation for a supersonic nozzle. Air mass flow rates at the secondary flow inlet and at the ejector discharge are derived from differential pressure gauges attached to pitot tubes plus measurements of air pressure and temperature.

A test section based on a 10 segment ejector subassembly was fabricated to evaluate performance characteristics. The test section consists of an 18 degree segment of the ejector with a stabilizer fin segment. The test section geometry and major dimensions are shown in Figure 8. A photograph of the test section showing the primary throat and mixing duct is provided in Figure 9. The test section incorporates clear sides to allow visualization of flow in the ejector.

SIMULATOR TEST RESULTS

An ejector test procedure was designed to explore the ejector operating surface defined in Figure 6. Ejector performance is maximized when the mass flow ratio is a maximum at pressure ratios of 1.2 to 1.3. Ejector performance tests were carried out at constant primary pressures ranging from 100 to 200 psi. At the local atmospheric pressure of 14.7 psi, with the inlet open to the atmosphere, these correspond to primary/secondary pressure ratios of 6.8 to 13.6. The tests were carried out by increasing the pressure ratio using the discharge throttle valve and observing the mass flow ratio.

Low Pressure Configuration

The ejector mixing duct opening, throat size and mixing duct length were first varied to obtain the best performance curves at a primary pressure ratio of 10. The performance of this low pressure configuration is shown in Figure 10. The mass flow ratio is relatively constant at low pressure ratios and drops steeply at high pressure ratios. The performance for a primary pressure ratio of 10.2 shows that the ejector can provide a mass flow ratio greater than 1 at pressure ratios of up to 1.2. At lower primary pressures, the mass flow ratio is higher but drops more quickly as the pressure ratio increases. At higher pressure, the mass flow ratio is more constant but has a lower value.

Partial Vacuum

A series of tests were conducted under partial vacuum conditions to verify theoretical predictions that the absolute pressure will not affect performance. These partial vacuum tests were carried out by using a choke on the secondary inlet to reduce the secondary pressure to 12.0 psia. The results of tests under partial vacuum (12.0 psia) are compared with atmospheric

pressure (14.7 psia) results in Figure 11. The mass flow ratios are essentially unaffected by the absolute value of secondary pressure. This results confirms that data taken at atmospheric pressure in the test stand can be used to predict ejector pressure and mass flow ratios at the higher altitude found at Yucca Mountain.

Stabilizer Fin Clearance

The dual wall drill string is constructed from mechanical tubing with a diameter of 6.000" plus or minus .045". The diameter tolerance requires that the ejector outer diameter must be 5.955" or less. The gap between the stabilizer fins and the dual wall allows some air to recirculate reducing the mass flow ratio. Ejector tests were carried out with a fin clearance spacing of .0625" and .125" to evaluate the effects on performance. The results, illustrated in Figure 12, show that these gap spacings have little effect on ejector performance at pressure ratios of 1.2 to 1.3. At higher pressure ratios, in the mixed flow regime, the mass flow ratio is significantly reduced. The presence of the gap actually increases the mass flow ratio at low pressure ratios indicating that air is entrained up though the gap.

Primary Throat Size

A critical parameter in sizing the ejector is the ratio of primary throat area to mixing duct area. The low pressure configuration used a throat area ratio of .075 based on Dutton and Carrol's (1986) design curves for a primary pressure ratio of 10. A variety of smaller throat openings were tested at higher pressures in an attempt to maximize the mass flow ratio at a pressure boost of 20%. The mass flow ratios, shown in Figure 13, clearly indicate an improvement in performance as the primary throat size decreases, with a breakdown in performance below a critical throat size. The best performance was achieved at the highest pressure ratio and smallest throat opening, giving a mass flow ratio of 1.2. The high pressure performance surface is shown in Figure 14.

Entrained Solids

The effect of adding cuttings to the secondary air flow was tested in the simulator by adding garnet sand to the secondary air flow at a concentration equivalent to coring with the dry drilling system at 43 ft/hr. In the test illustrated in Figure 16, the pressure ratio was set to 20%. When the sand is added, the secondary air flow drops significantly then climbs to a relatively steady state value. The addition of the sand causes the secondary mass flow ratio to drop to 1.1 but the total mass flow ratio, including cuttings increases substantially. The sand had essentially no effect on pressure ratio.

A measurement of the air velocity distribution in the mixing duct showed how the mass flow ratio can increase when particles are added to the flow. The mixing duct stagnation pressure was profiled across the width of the duct, at the mixing duct exit, using a static pressure tube. The stagnation pressure profile, shown in Figure 18, indicates a high speed wall jet strongly attached to the inner wall of the mixing duct. Figure 19 shows the trajectories of fluorescent polystyrene beads added to the flow and illuminated by a sheet of laser light. The particles bounce off of the inner wall of the mixing duct where they enter the attached wall jet. Enhanced momentum transfer to particles in the wall jet can account for the increased mass flow ratio observed when particles are added to the flow.

CONCLUSIONS

The design study has shown that a segmented annular ejector with sufficient clearance to fit inside of a dual wall drill string designed for dry air drilling can provide a significant vacuum boost on the hole bottom during coring operations. A segmented annular ejector design capable of providing a 20% pressure boost under realistic operating conditions at a mass flow ratio of 1.1 or better was demonstrated using a laboratory simulator. The ejector performance characteristics can be adjusted to maximize pressure boost or mass flow ratio, by changing the primary nozzle size for low or high pressure operation. The addition of particles to the entrained flow enhances the ejector performance. The pressure boost provided by an ejector subassembly would increase the depth capacity of the dry drilling system by 60% and provide a much greater margin of safety during coring operations.

ACKNOWLEDGMENTS

This work was supported by the DoE Yucca Mountain Project. The support and encouragement of Roy Long, Eddie Wright and Greg Fehr are gratefully acknowledged. Prof. Craig Dutton provided the CAEOPT3 code used to size the ejector.

REFERENCES

Dutton, J.C. and B.F. Carrol (1986) "Optimal supersonic ejector designs," *J. Fluids. Eng.*, 108, 414-420.

Kolle, J.J. (1993) "Ejector Subassembly Feasibility Analysis, " *QUEST Technical Report No 614*, QUEST Integrated Inc., Kent Washington.

Long, R., D. Wonderly and E. Wright (1992) "A drilling and coring system for studying unsaturated zone in-situ conditions," *PDE-Vol. 40, Drilling Technology*, ASME, New York.

Lyons W.C. (1984) *Air and Gas Drilling Manual*, Gulf Publishing Co., Houston Texas.

Rundstadler, P.W., F.X. Dolan, and R.C. Dean (1975) *Diffuser Data Book, TN-186*, Creare Inc., Hanover, New Hampshire.

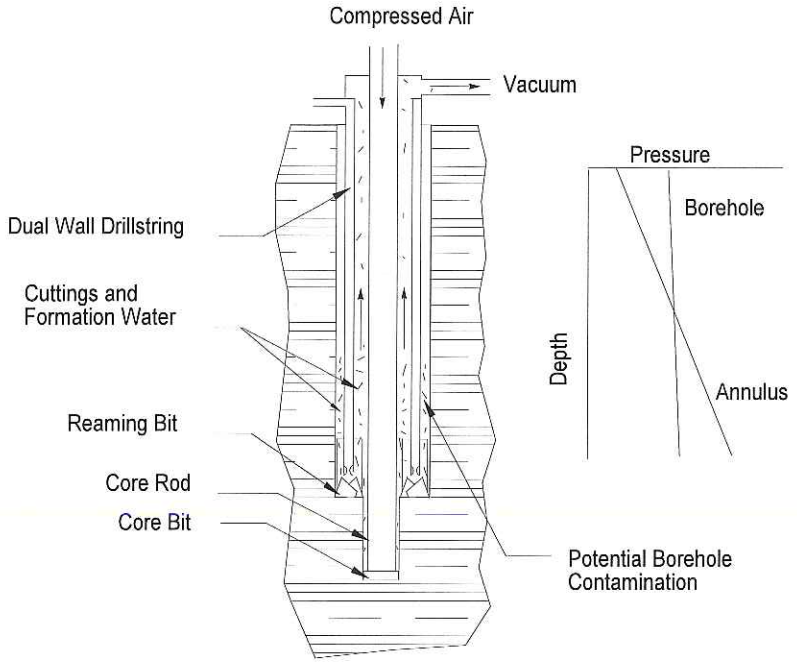

Figure 1. Potential borehole contamination during coring with dry drilling system.

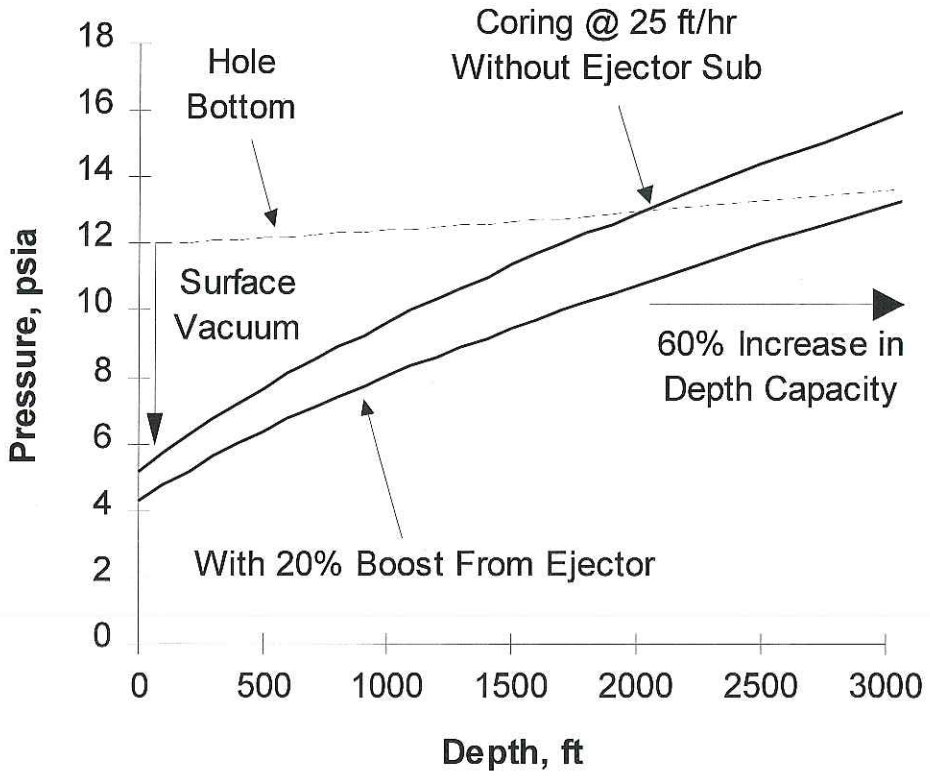

Figure 2. Dry drilling system pressures.

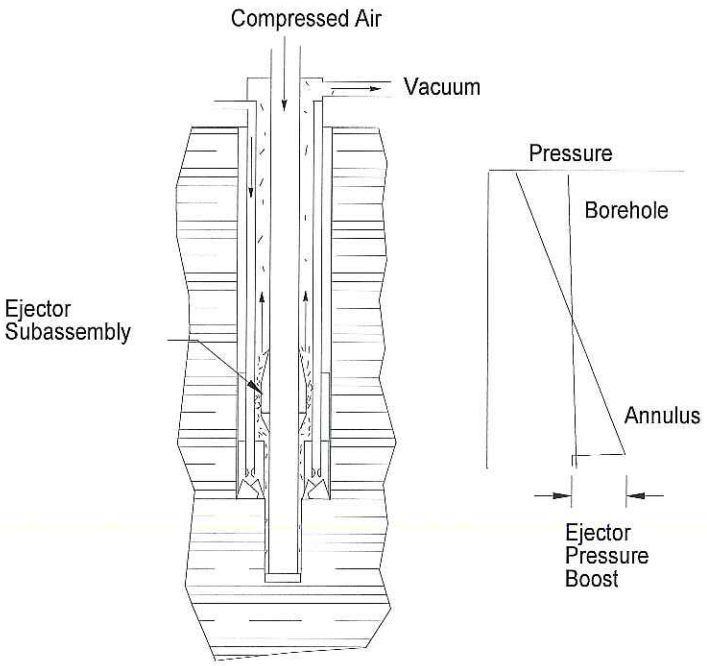

Figure 3. Ejector subassembly concept.

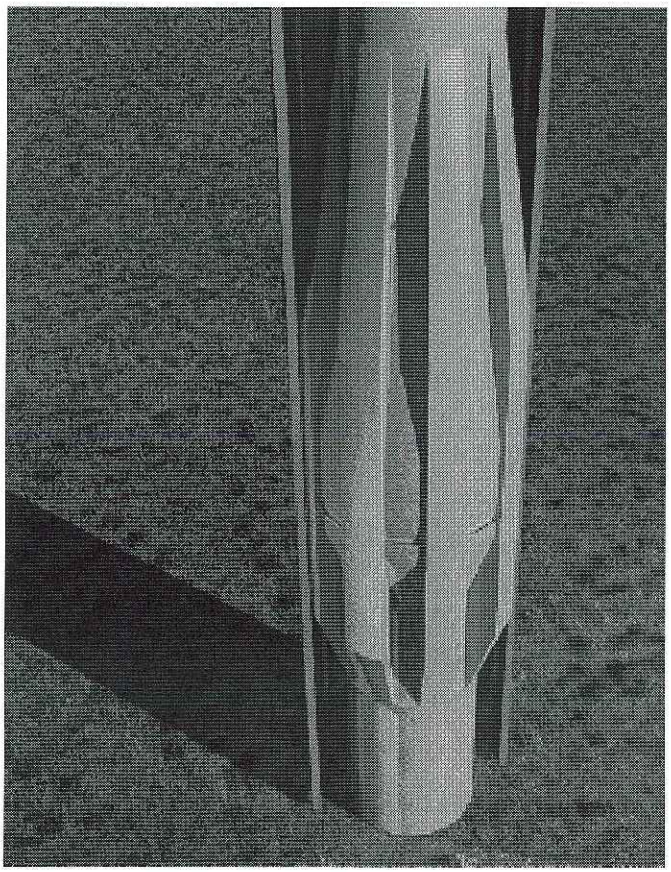

Figure 4. Segmented annular ejector design..

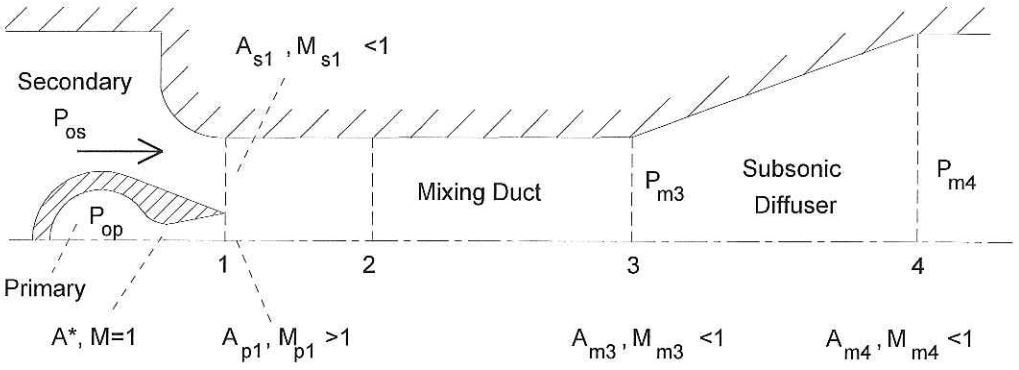

Figure 5. Ejector geometry and definitions.

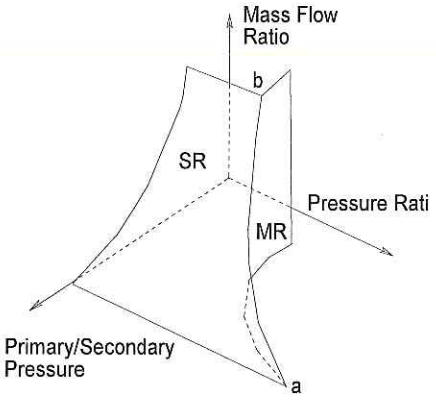

Figure 6. Ejector operating surface.

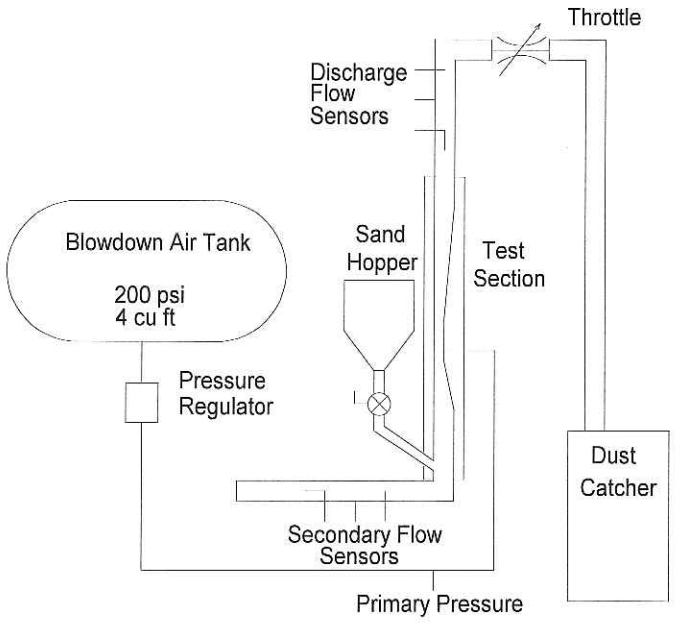

Figure 7. Ejector simulator schematic.

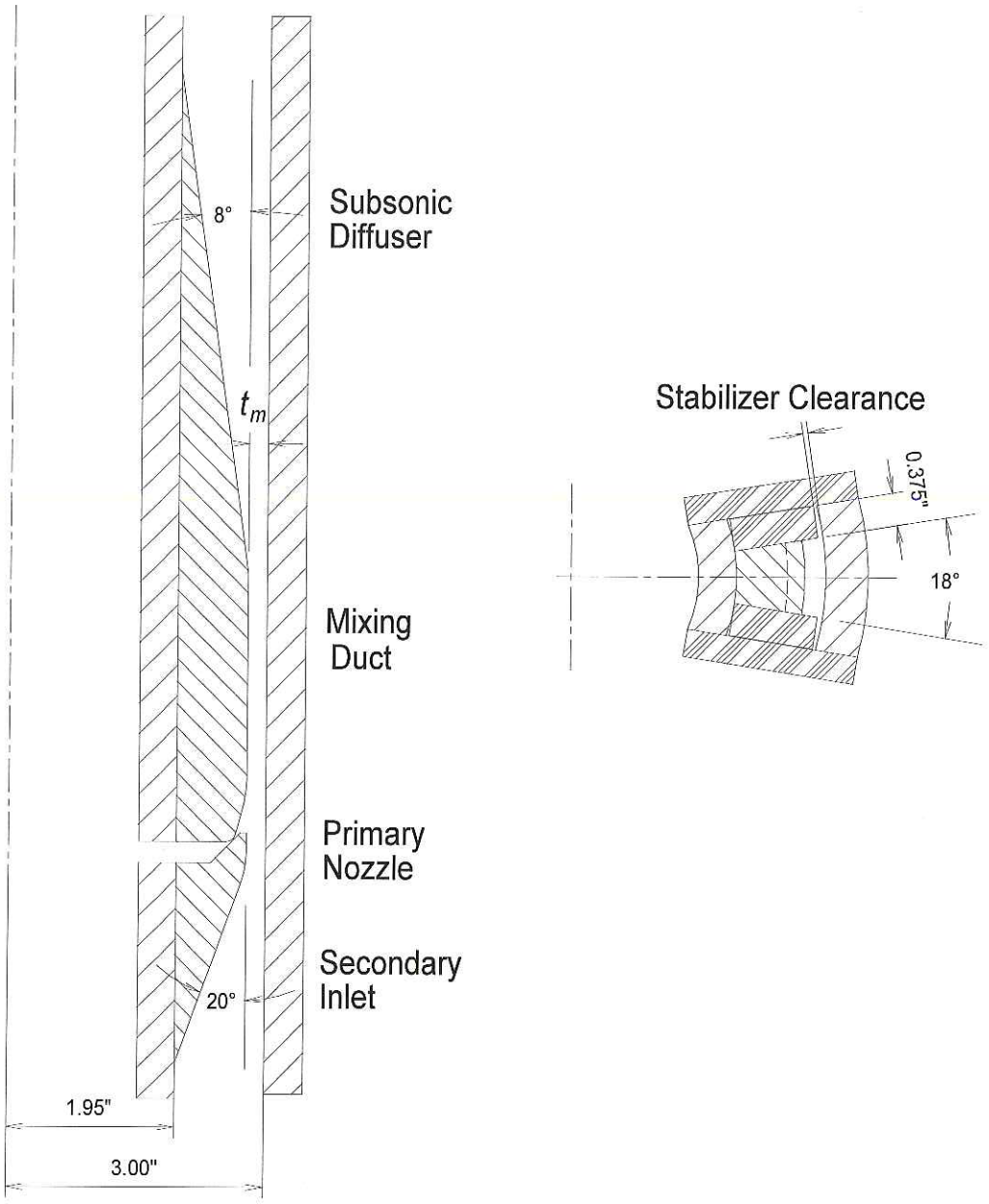

Figure 8. Simulator test section geometry.

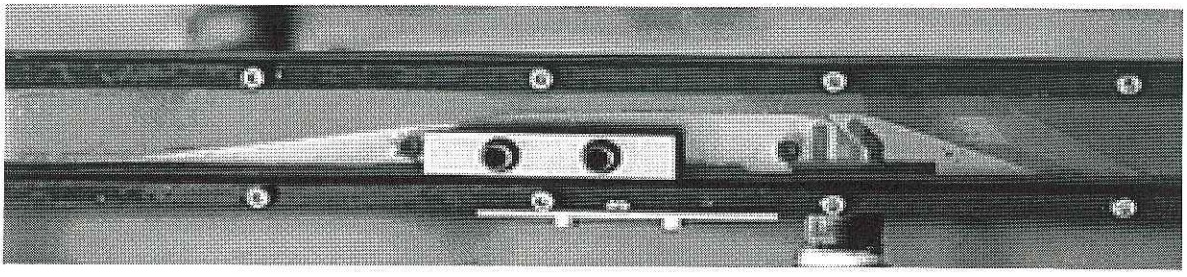

Figure 9. Ejector test section.

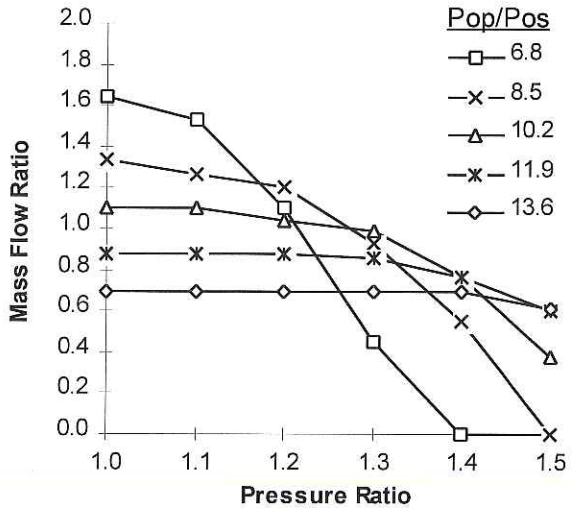

Figure 10. Low pressure configuration ejector performance surface.

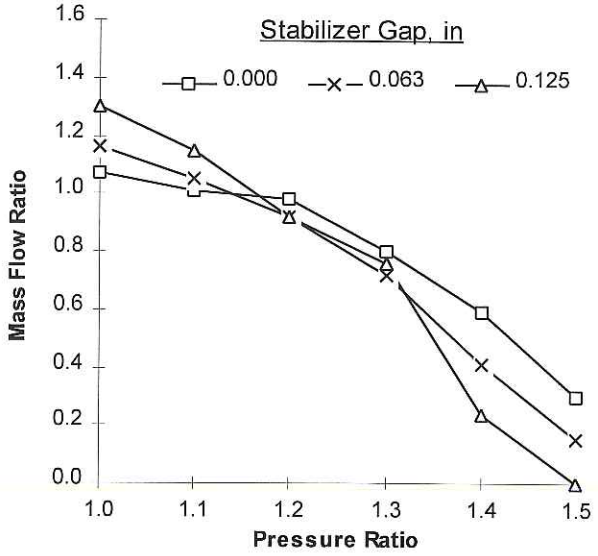

Figure 12. Effects of stabilizer clearance gap on performance.

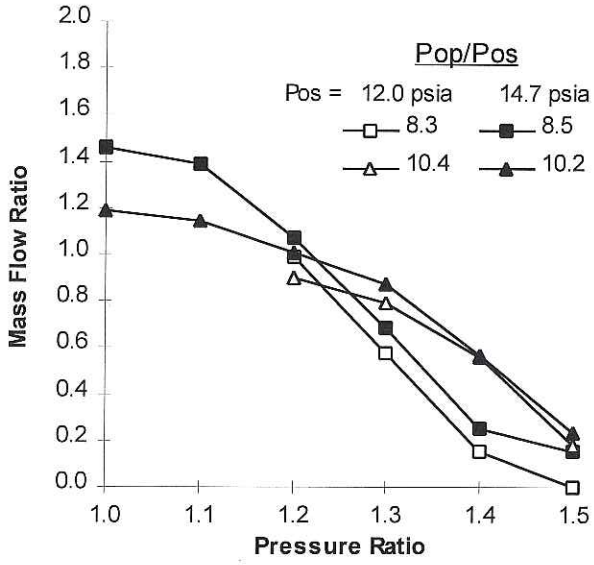

Figure 11. Effect of secondary pressure.

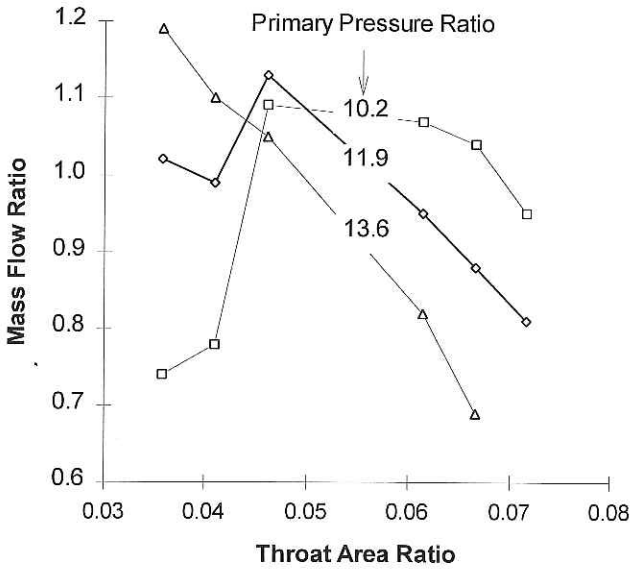

Figure 13. Primary throat area ratio effects

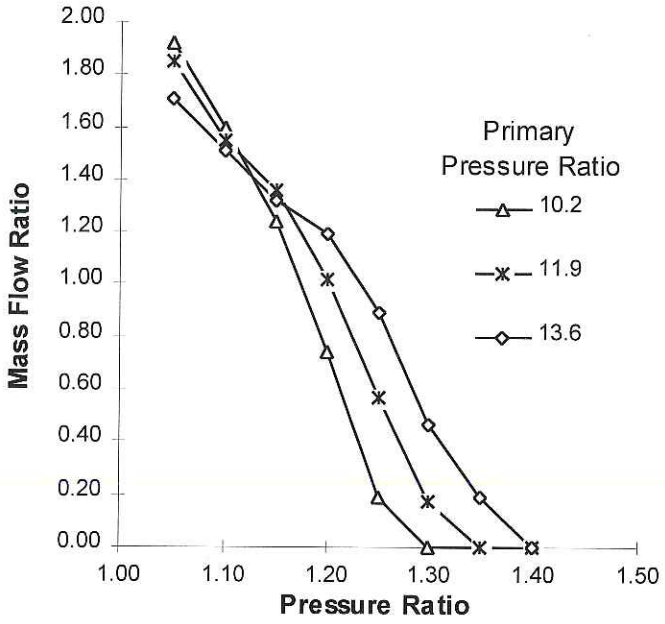

Figure 14. High pressure configuration performance surface.

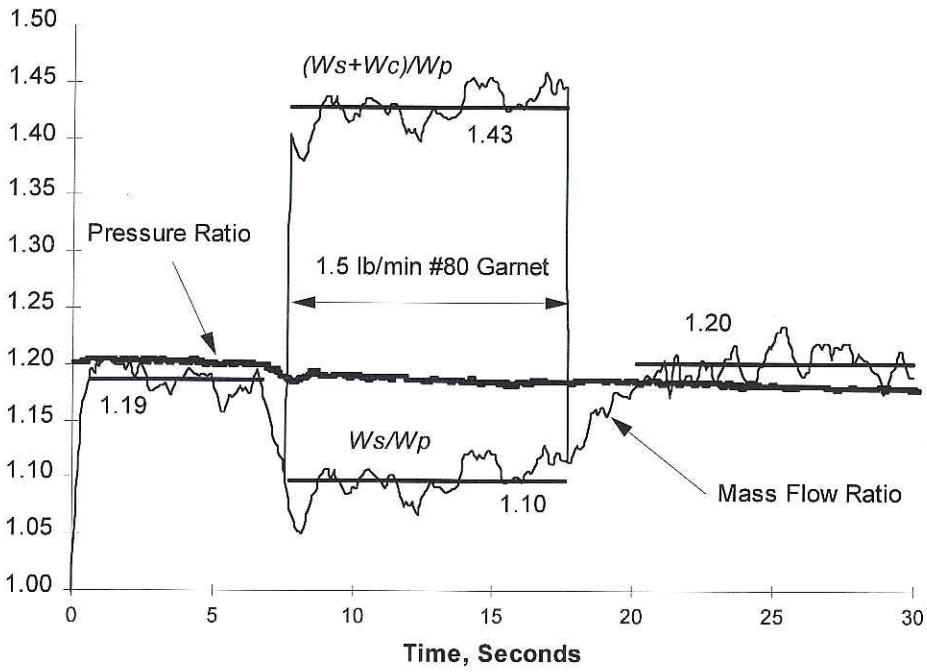

Figure 15. Effects of cuttings addition on secondary air flow ratio.

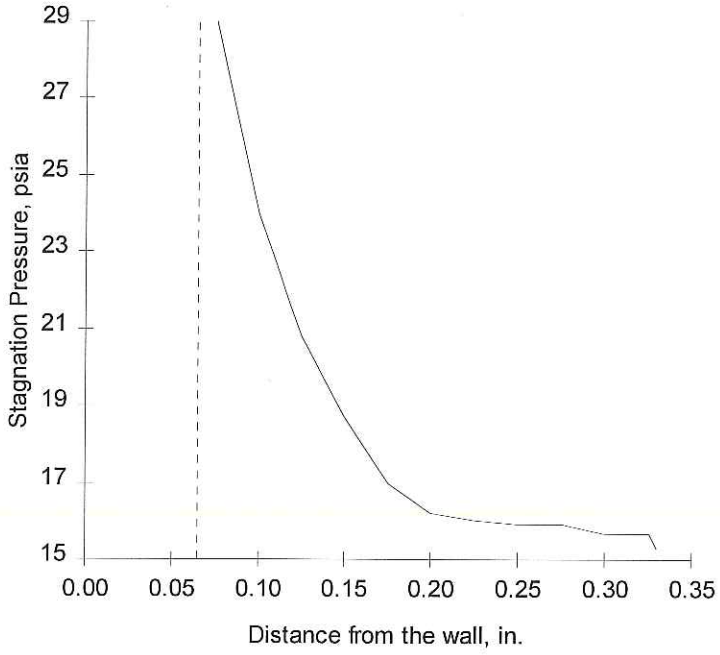

Figure 16. Mixing duct stagnation pressure profile.

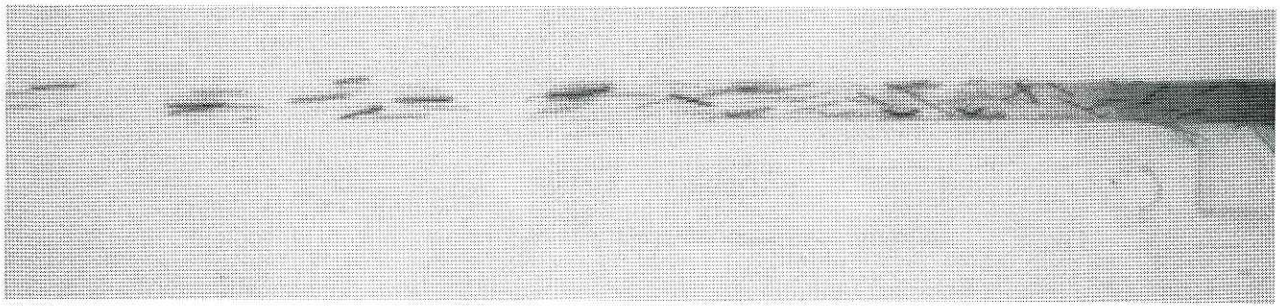

Figure 17. Visualization of fluorescent beads in the mixing duct.